

PCCP

Accepted Manuscript



This is an *Accepted Manuscript*, which has been through the Royal Society of Chemistry peer review process and has been accepted for publication.

Accepted Manuscripts are published online shortly after acceptance, before technical editing, formatting and proof reading. Using this free service, authors can make their results available to the community, in citable form, before we publish the edited article. We will replace this *Accepted Manuscript* with the edited and formatted *Advance Article* as soon as it is available.

You can find more information about *Accepted Manuscripts* in the [Information for Authors](#).

Please note that technical editing may introduce minor changes to the text and/or graphics, which may alter content. The journal's standard [Terms & Conditions](#) and the [Ethical guidelines](#) still apply. In no event shall the Royal Society of Chemistry be held responsible for any errors or omissions in this *Accepted Manuscript* or any consequences arising from the use of any information it contains.



PCCP

COMMUNICATION

NMR Reveals the Surface Functionalisation of Ti_3C_2 MXene

Michael A. Hope^a, Alexander C. Forse^a, Kent J. Griffith^a, Maria R. Lukatskaya^b, Michael Ghidui^b, Yury Gogotsi^{b,*}, Clare P. Grey^{a,*}

Received 00th January 20xx,
Accepted 00th January 20xx

DOI: 10.1039/x0xx00000x

www.rsc.org/

1H and ^{19}F NMR experiments have identified and quantified the internal surface terminations of $Ti_3C_2T_x$ MXene. Ti-F and Ti-OH terminations are shown to be intimately mixed and there are found to be significantly fewer -OH terminations than -F and O, with the proportions highly dependent on the synthesis method.

MXenes are a novel class of two-dimensional transition metal carbides and nitrides^{1,2} which have garnered much interest for applications in lithium-ion³ and Li-S⁴ batteries, supercapacitors⁵, selective adsorption of heavy ions⁶, and dual response systems⁷. They are synthesised by etching the 'A' element out of the corresponding MAX phase; for example, the most widely studied MXene, and that which this work is based on, Ti_3C_2 , is produced by etching Al out of Ti_3AlC_2 (Figure 1a).

Aqueous etching of Al does not leave bare Ti layers, but they are instead terminated with functional groups (T), with the material then referred to as $Ti_3C_2T_x$. X-ray photoelectron spectroscopy (XPS) experiments have indicated the presence of O, OH and F terminations^{3,8} and energy-dispersive X-ray spectroscopy (EDS) has been used to quantify their proportions^{2,9,10}; however, EDS cannot distinguish between O and OH and typically all O is assumed to be present as OH. The analysis is further complicated by the presence of interlayer water and etching by-products, such as fluoride salts, that are often spuriously included in the signals assigned to surface termination.

In many studies it has been necessary either to assume average site occupancies for the functional groups, for example to analyse pair distribution functions⁹, or to simply use complete termination of one type as assumed for density functional theory (DFT) calculations^{2,11–13}. Moreover, DFT calculations have suggested that the electronic properties¹¹ and

performance of MXenes in lithium-ion batteries^{12,13} are highly dependent on the surface functionalisation, so a greater understanding is crucial for pursuing the aforementioned applications. It is clear that a more complete understanding of the surface functionalisation of these interesting materials would aid their development for applications.

In this work, nuclear magnetic resonance (NMR) spectroscopy is used to study the surface functionalisation of $Ti_3C_2T_x$. NMR is a powerful tool for studying fluorine and hydrogen containing materials due to the high sensitivity of ^{19}F and 1H nuclei¹⁴, and has recently been applied to study another MXene, V_2CT_x ¹⁵. While V_2CT_x remains the only MXene thus far characterized by NMR, $Ti_3C_2T_x$ is the most studied MXene and has already demonstrated promise in many applications. In the original procedure, etching was performed with 50% HF solution², but more recently a new synthesis has been reported¹⁰ using a milder etchant, LiF dissolved in 6M HCl, which is safer and produces $Ti_3C_2T_x$ with a lower concentration of defects and a higher volumetric capacitance when used in an aqueous supercapacitor. Samples prepared by the two methods are compared here.

Some differences between the preparations are evident: scanning electron microscopy (SEM) shows that, while HF-etched samples have an accordion-like morphology (Figure 1b), the samples etched with LiF and HCl mixtures show a more compact structure (Figure 1c) without visible delaminations. X-ray diffraction (XRD) showed a shift in the (0002) reflection to lower angles (corresponding to a *c* parameter of ~25 Å) for LiF-HCl etched samples (Figure 1d), compared to HF-etched MXene on the order of 19-20 Å. However, there is evidence of small amounts of unreacted Ti_3AlC_2 in the LiF-HCl etched sample.

These observations correspond well with the ^{13}C NMR data (Figure 2a) which provides further evidence for the conversion of Ti_3AlC_2 to $Ti_3C_2T_x$ (although these spectra are not quantitative, due to the faster transverse relaxation time, T_2 , of $Ti_3C_2T_x$ compared to Ti_3AlC_2). The Ti_3AlC_2 shows a resonance at 566 ppm with a shoulder at 527 ppm ascribed to TiC remaining from the synthesis¹⁶. For the LiF-HCl synthesised

^a Department of Chemistry, University of Cambridge, Lensfield Road, Cambridge CB2 1EW, UK.

^b Department of Materials Science and Engineering, and A.J. Drexel Nanomaterials Institute, Drexel University, Philadelphia, PA 19104, USA.

*corresponding authors: gogotsi@drexel.edu and cpg27@cam.ac.uk

Electronic Supplementary Information (ESI) available: Experimental details, additional NMR spectra and EDS analysis of the $Ti_3C_2T_x$ samples.

See DOI: 10.1039/x0xx00000x

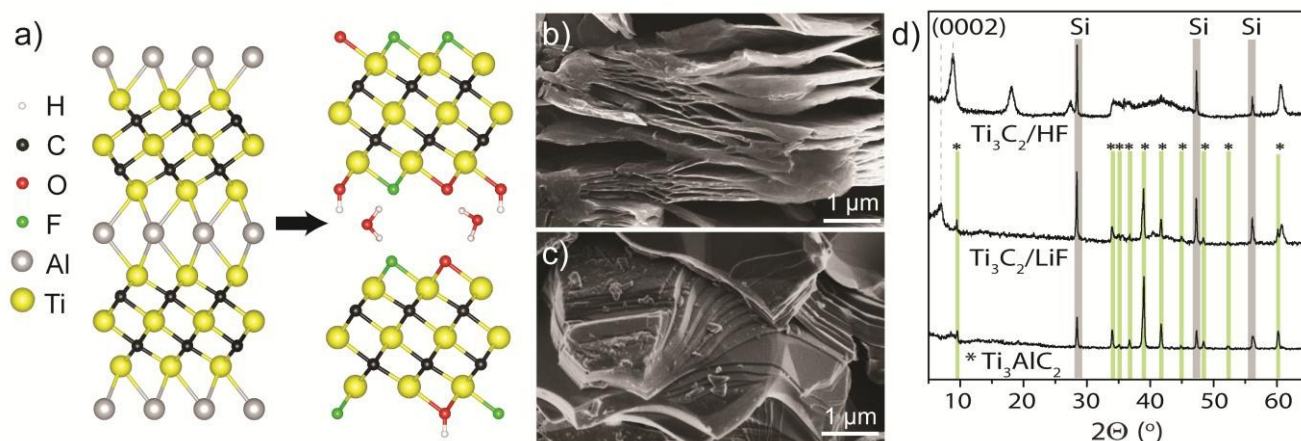


Figure 1: a) Schematic of etching from Ti_3AlC_2 to $\text{Ti}_3\text{C}_2\text{T}_x$ showing terminations and interlayer water. Typical SEM micrographs of (b) HF-etched $\text{Ti}_3\text{C}_2\text{T}_x$, showing accordion-like structure and (c) LiF-HCl etched $\text{Ti}_3\text{C}_2\text{T}_x$, with a more compact structure. d) XRD patterns of Ti_3AlC_2 and $\text{Ti}_3\text{C}_2\text{T}_x$ etched with HF or LiF-HCl. Green vertical lines denote the presence of MAX phase peaks, and grey regions are peaks from crystalline Si 10 wt % internal standard.

sample, the Ti_3AlC_2 signal reduces in intensity relative to the TiC signal as Ti_3AlC_2 is converted to $\text{Ti}_3\text{C}_2\text{T}_x$, and a new resonance appears at 412 ppm, attributed to $\text{Ti}_3\text{C}_2\text{T}_x$. For the HF synthesis, conversion is complete and the main $\text{Ti}_3\text{C}_2\text{T}_x$ resonance now appears at 382 ppm, the shift difference being most likely due to a difference in surface functionalisation or stacking. In comparison, the ^{13}C signals in V_2AlC and V_2CT_x were found at lower chemical shifts of 208 ppm and 265 ppm respectively. The larger ^{13}C chemical shifts seen in the Ti system compared to the V system are in part ascribed to larger overlap between Ti and C due to the larger, more diffuse Ti orbitals.

Initial ^1H NMR experiments on the as-synthesised materials showed only an intense resonance at 6.9 ppm due to water (see Supp. Info.), but after drying at 200 °C *in vacuo* overnight, different proton environments could be distinguished (Figure 2b). The HF synthesised sample shows a broad signal at 18.6 ppm with a similar signal seen for the LiF-HCl synthesised sample at 12.5 ppm. These are assigned to Ti-OH terminations with varying degrees of hydrogen bonding. Both ^1H spectra also show a feature at 6.5 ppm, ascribed to H_2O as its intensity was sensitive to the degree of drying, suggesting that water trapped between the MXene layers cannot be completely removed by vacuum drying at 200 °C. The other proton signals observed between 3 and -1.5 ppm are tentatively assigned to intercalated contaminants as the intensities and chemical shifts were found to vary between different samples.

To confirm the connectivity of the -OH groups to the Ti_3C_2 sheets, a two-dimensional ^1H - ^{13}C heteronuclear correlation (HETCOR) spectrum was recorded for the HF synthesised sample (Figure 2c). These experiments show correlations only for species in close proximity, on the order of angstroms¹⁷. Although the spectrum is broad, the Ti-OH terminations at δ ^1H ~20 ppm clearly correlate with the Ti_3C_2 carbon environment at δ ^{13}C ~380 ppm, confirming the connectivity. The absence of the other ^1H signals in this spectrum indicates the environments are further from the carbon layers and/or highly mobile, i.e. intercalants, not surface terminations.

The large ^1H chemical shifts in these systems, outside the normal ^1H chemical shift range, could arise from three major sources: the Knight shift, due to metallic behaviour; a transferred hyperfine (or Fermi contact) shift due to the transfer of (unpaired) spin density from the Ti layers; and/or strong hydrogen bonding. The prior NMR study on V_2CT_x , revealed V-OH terminations with much larger ^1H chemical shifts of 85 ppm, the shifts being ascribed to Knight shifts due to the metallic/low band gap V_2CT_x ¹⁵. A ^1H saturation recovery experiment on $\text{Ti}_3\text{C}_2\text{T}_x$ yielded a T_1 relaxation constant of ~3 s for the Ti-OH signal, whereas hyperfine interactions should cause fast T_1 relaxation; in contrast, V-OH terminations in V_2CT_x have T_1 ~ 1 ms. Furthermore, variable temperature ^1H NMR experiments performed between -8 and 62 °C showed no appreciable change in chemical shift, as would be expected for a hyperfine shift. The large chemical shift of the Ti-OH terminations in $\text{Ti}_3\text{C}_2\text{T}_x$ is therefore most likely due to strong hydrogen bonding rather than a hyperfine shift, different H-bonding arrangements being observed for the two samples. However, a small contribution from the Knight shift cannot be ruled out, particularly since the observed chemical shifts are close to the maximum ^1H shift observed in strongly H-bonded systems¹⁸, and the presence of large shifts in the ^{13}C NMR spectra, which are likely caused by the Knight shift in metallic $\text{Ti}_3\text{C}_2\text{T}_x$.

In the ^{19}F spectra (Figure 2d), broad signals are observed at -227 ppm in the HF synthesised sample and at -255 ppm in the LiF-HCl synthesised sample, which are assigned to Ti-F terminations. The LiF-HCl synthesised sample also shows residual LiF at -203 ppm¹⁹ and the reaction by-product $\text{AlF}_3 \cdot n\text{H}_2\text{O}$ at -181 ppm²⁰, which could be removed by stirring overnight in water. In the HF synthesised sample, the $\text{AlF}_3 \cdot n\text{H}_2\text{O}$ has shifted to -166 ppm, likely due to differences in hydration; there is a resonance at 8 ppm most probably due to TiF_3 produced in the harsher etching conditions (see Supp. Info. for TiF_3 spectrum), and a broad signal at -100 ppm which may be due to a fluorinated hydrocarbon or metal oxyfluoride contaminant. This is very comparable to the V_2CT_x MXene

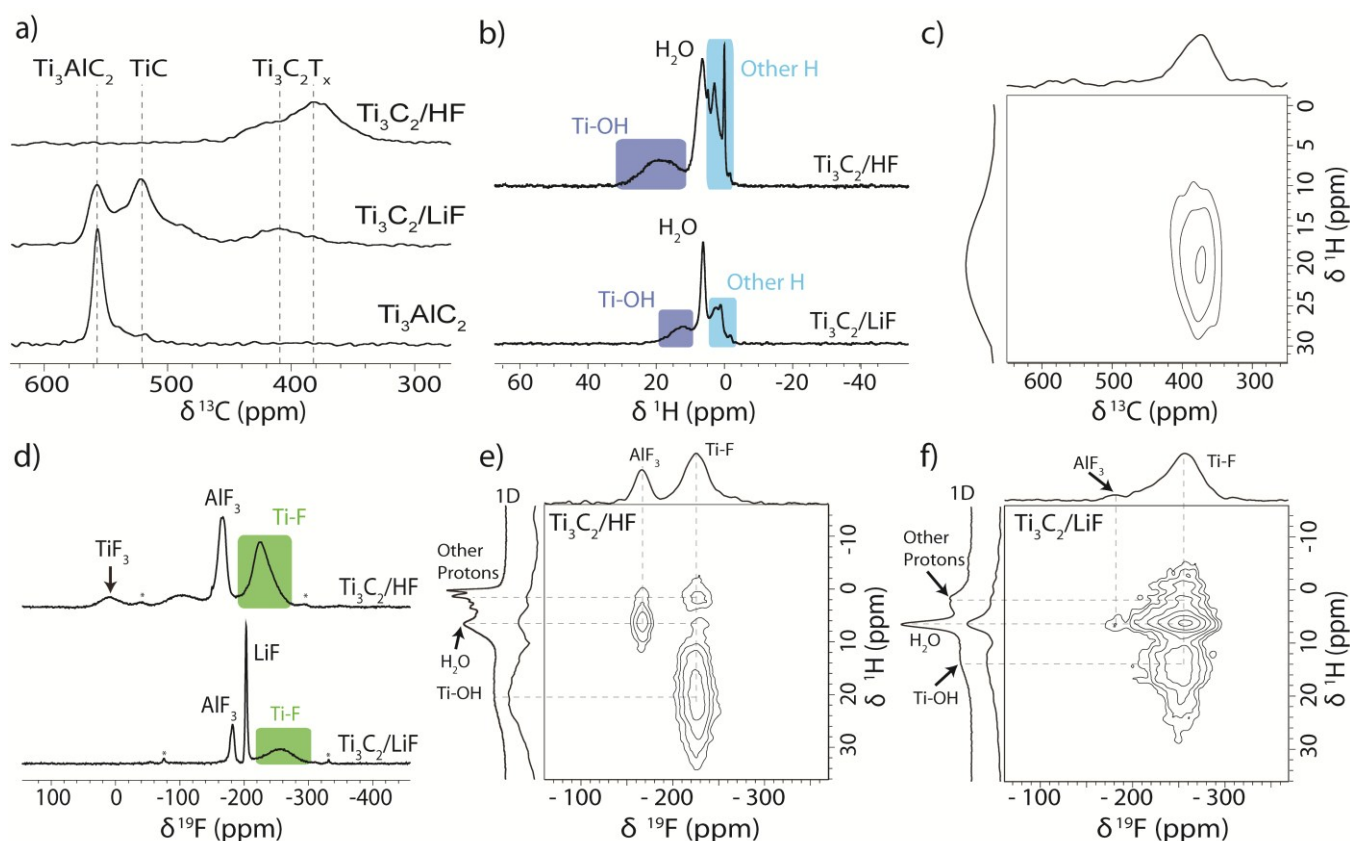


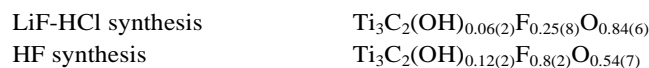
Figure 2: a) ^{13}C NMR (11.7 T) spectra of Ti_3AlC_2 and $\text{Ti}_3\text{C}_2\text{T}_x$ produced by the two methods recorded at 50 kHz MAS using a Carr-Purcell-Meiboom-Gill (CPMG) experiment with the echoes summed to give the conventional lineshape (see Supp. Info.). b) ^1H NMR (11.7 T) spectra of HF and LiF-HCl synthesised Ti_3C_2 MXene recorded at 60 kHz MAS. c) ^1H - ^{13}C HETCOR NMR (7.05 T) spectrum of HF synthesised Ti_3C_2 MXene recorded at 40 kHz MAS. d) ^{19}F NMR (11.7 T) spectra of HF and LiF-HCl synthesised Ti_3C_2 MXene recorded at 60 kHz MAS. ^1H - ^{19}F HETCOR NMR (11.7 T) spectra of e) HF and f) LiF-HCl synthesised Ti_3C_2 MXene recorded at 20 kHz MAS with adjacent 1D ^1H spectra shown for comparison.

system where V-F terminations are observed at -265 ppm, an AlF_3 like species at -158 ppm and a contaminant at -122 ppm.

To explore the arrangement of the different functional groups in space, ^1H - ^{19}F HETCOR spectra were also recorded (Figures 2e and f). The correlation between Ti-OH and Ti-F terminations in both samples confirms our spectral assignments and reveals there are mixed terminations within layers, rather than regions terminated by a single type of functional group. The correlation between H_2O and Ti-F terminations is indicative of structural water between the layers; the stronger correlation in the LiF-HCl etched sample may suggest the water is less mobile, but further experiments with varied contact times would be required to confirm this. The other ^1H signals centred at $\delta^1\text{H}$ 1 ppm also correlate with the Ti-F resonance, supporting the assertion that these arise from intercalated species and finally, there is H_2O and AlF_3 correlation due to the hydration of AlF_3 .

Having identified Ti-OH and Ti-F surface functional groups, their proportions were quantified by spin counting (comparing the signal with that of a known standard), correcting for the mass of known impurities and the percentage conversion of the LiF-HCl synthesised sample as determined by EDS (see Supp. Info.). The fraction of oxygen terminations is then determined by assuming that there are two terminations per formula unit (one per side) and that oxygen comprises the remainder. We further assume that oxygen takes up two sites,

because it most likely originated from two Ti-OH groups ($-\text{OH} + -\text{OH} \rightarrow \text{O} + \text{H}_2\text{O}^{21}$) and has a greater negative charge; i.e. the following equation is satisfied: $n_{\text{OH}} + n_{\text{F}} + 2n_{\text{O}} = 2$. This yields the following formulae (Figure 3); the error in the last digit is shown in brackets:



This reveals that the Ti-OH termination is a relatively minor component, with far more Ti-F and Ti-O present. 2D ^1H NMR spectra corroborate this by showing there are no -OH terminations next to -OH terminations (see Supp. Info.) and recent quantitative XPS results⁸ are also in strong agreement. However, this result differs from the stoichiometries deduced from previous EDS experiments due to their assumption that all O is present as -OH terminations and because the enduring presence of H_2O and fluoride containing impurities significantly affects the O:F ratio. There is also a clear difference between the functional groups of the samples prepared by HF and LiF-HCl syntheses; there is almost four times as much -F termination in the HF synthesised sample, as well as more -OH and we conclude there must therefore be fewer O terminations. High content of O-terminated titanium atoms and a low content of -OH and -F terminal groups in LiF-HCl etched samples suggests that this method is preferred for

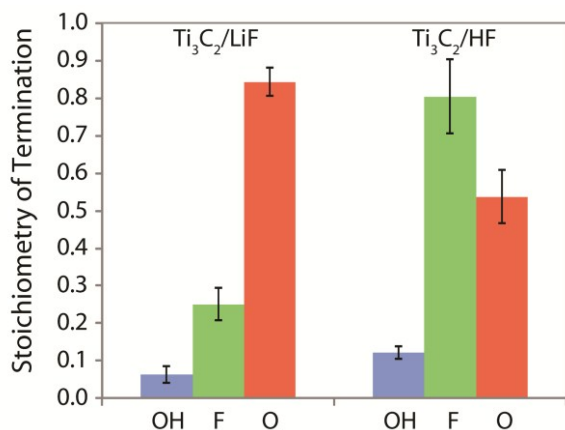


Figure 3: Composition of the $\text{Ti}_3\text{C}_2\text{T}_x$ surface functional groups produced by etching of the Ti_3AlC_2 in HF and LiF-HCl solutions, per Ti_3C_2 formula unit, i.e. $\text{Ti}_3\text{C}_2(\text{OH})_x\text{F}_y\text{O}_z$.

producing MXenes for Li-ion and other batteries where O-termination gives a higher capacity¹², although complete conversion is not achieved.

It was considered that vacuum drying could have caused the conversion of Ti-OH terminations to O according to $-\text{OH} + -\text{OH} \rightarrow \text{O} + \text{H}_2\text{O}$ ²¹, and hence the low levels of Ti-OH terminations observed. Using a long spin-echo as a T_2 filter it was possible to largely remove the H_2O signal in the ^1H NMR spectrum and resolve the Ti-OH terminations before drying. A comparison of the spectra before and after drying *in vacuo* at 200 °C showed no change in Ti-OH intensity and therefore the termination proportions determined for vacuum dried samples are also valid for the material as synthesised (see Supp. Info.).

In conclusion, Ti-OH and Ti-F terminations have been identified in the ^1H and ^{19}F NMR spectra of $\text{Ti}_3\text{C}_2\text{T}_x$ MXene, as well as H_2O still present between the $\text{Ti}_3\text{C}_2\text{T}_x$ sheets after vacuum drying at 200 °C. Two-dimensional correlation experiments have confirmed the connectivity of the Ti-OH and Ti-F terminations and revealed that they are all present in close vicinity to each other between the metal carbide layers. Quantitative NMR experiments then showed that there are significantly fewer -OH terminations than -F and O terminations and that the surface termination is highly sensitive to the synthesis method used; in particular the HF synthesised material has almost four times as much -F termination as the LiF-HCl synthesised material. Our measurements give a new level of insight into the chemistry of these exciting materials, and should facilitate their development in electrochemical energy storage applications. We also note that the NMR methods used here are generally applicable to the large family of MXene compounds.

We are grateful for financial support by the Oppenheimer Foundation and EPSRC. We would like to thank Professor M. W. Barsoum, Drexel University, for helpful discussions; Chang E. Ren, Drexel University, for help with material characterization; and Zigeng Liu and Yan-Yan Hu, Cambridge University, for providing the ^{19}F NMR of TiF_3 . Material synthesis and characterization at Drexel University was supported by the US National Science Foundation under grant

number DMR-1310245. The experimental data for all NMR experiments has been made available at www.repository.cam.ac.uk/handle/1810/253254.

Notes and references

- M. Naguib, V. N. Mochalin, M. W. Barsoum and Y. Gogotsi, *Adv. Mater.*, 2014, **26**, 992–1005.
- M. Naguib, M. Kurtoglu, V. Presser, J. Lu, J. Niu, M. Heon, L. Hultman, Y. Gogotsi and M. W. Barsoum, *Adv. Mater.*, 2011, **23**, 4248–4253.
- O. Mashtalir, M. Naguib, V. N. Mochalin, Y. Dall’Agnese, M. Heon, M. W. Barsoum and Y. Gogotsi, *Nat. Commun.*, 2013, **4**, 1716.
- X. Liang, A. Garsuch and L. F. Nazar, *Angew. Chem. Int. Ed.*, 2015, **54**, 3907–3911.
- M. R. Lukatskaya, O. Mashtalir, C. E. Ren, Y. Dall’Agnese, P. Rozier, P. L. Taberna, M. Naguib, P. Simon, M. W. Barsoum and Y. Gogotsi, *Science*, 2013, **341**, 1502–5.
- Q. Peng, J. Guo, Q. Zhang, J. Xiang, B. Liu, A. Zhou, R. Liu and Y. Tian, *J. Am. Chem. Soc.*, 2014, **136**, 4113–4116.
- J. Chen, K. Chen, D. Tong, Y. Huang, J. Zhang, J. Xue, Q. Huang and T. Chen, *Chem. Commun.*, 2015, **51**, 314–317.
- J. Halim, K. M. Cook, M. Naguib, P. Eklund, Y. Gogotsi, J. Rosen and M. W. Barsoum, *Appl. Surf. Sci.*, 2016, **362**, 406–417.
- C. Shi, M. Beidaghi, M. Naguib, O. Mashtalir, Y. Gogotsi and S. J. L. Billinge, *Phys. Rev. Lett.*, 2014, **112**, 125501.
- M. Ghidui, M. R. Lukatskaya, M.-Q. Zhao, Y. Gogotsi and M. W. Barsoum, *Nature*, 2014, **516**, 78–81.
- M. Khazaei, M. Arai, T. Sasaki, C.-Y. Chung, N. S. Venkataramanan, M. Estili, Y. Sakka and Y. Kawazoe, *Adv. Funct. Mater.*, 2013, **23**, 2185–2192.
- Y. Xie, M. Naguib, V. N. Mochalin, M. W. Barsoum, Y. Gogotsi, X. Yu, K. W. Nam, X. Q. Yang, A. I. Kolesnikov and P. R. C. Kent, *J. Am. Chem. Soc.*, 2014, **136**, 6385–6394.
- C. Eames and M. S. Islam, *J. Am. Chem. Soc.*, 2014, **136**, 16270–16276.
- K. J. MacKenzie and M. E. Smith, *Multinuclear Solid-State Nuclear Magnetic Resonance of Inorganic Materials*, 2002.
- K. J. Harris, M. Bugnet, M. Naguib, M. W. Barsoum and G. R. Goward, *J. Phys. Chem. C*, 2015, 13713–13720.
- K. J. MacKenzie, R. H. Meinhold, D. G. McGavin, J. a Ripmeester and I. Moudrakovski, *Solid State Nucl. Mag.*, 1995, **4**, 193–201.
- S. R. Hartmann and E. L. Hahn, *Phys Rev*, 1962, **128**, 2042–2053.
- M. R. Chierotti and R. Gobetto, in *Supramolecular Chemistry: From Molecules to Nanomaterials.*, eds. J. W. Steed and P. A. Gale, Wiley, 2012, pp. 331–347.
- È. Grimmer, E. Kemnitz, U. Groû and S. Ru, *J. Fluor. Chem.*, 2002, **115**, 193–199.
- R. König, G. Scholz, a. Pawlik, C. Jager, B. Van Rossum and E. Kemnitz, *J. Phys. Chem. C*, 2009, **113**, 15576–15585.
- L. H. Karlsson, J. Birch, J. Halim, M. W. Barsoum and P. O. Å. Persson, *Nano Lett.*, 2015, 150715104328006.